Structure factor of compressed liquid deuterium close to the melting transition

M. Zoppi,[1] A. K. Soper,[2] R. Magli,[3,4] F. Barocchi,[4,5] U. Bafile,[1] and N. W. Ashcroft[6]
[1]*Consiglio Nazionale delle Ricerche, Istituto di Elettronica Quantistica, via Panciatichi 56/30, I-50127 Firenze, Italy*
[2]*Rutherford Appleton Laboratory, Neutron Science Division, Chilton, Didcot, Oxon, OX11 0QX, United Kingdom*
[3]*Dipartimento di Energetica, Università di Firenze, via di S. Marta 3, I-50139 Firenze, Italy*
[4]*Istituto Nazionale di Fisica della Materia, Unità di Ricerca di Firenze, Italy*
[5]*Dipartimento di Fisica, Università di Firenze, Largo E. Fermi 2, I-50125 Firenze, Italy*
[6]*Laboratory of Atomic and Solid State Physics and Materials Science Center, Cornell University, Ithaca, New York 14853-3501*
(Received 19 January 1996)

The structure factor of compressed liquid deuterium has been measured, using time-of-flight neutron diffraction, in five thermodynamic states close to the melting line. The pressure and temperature ranges were selected in the intervals $p=48.5-467$ bar and $T=20.7-29.0$ K, respectively. The highest liquid density is close to that of the solid phase at the triple point. [S1063-651X(96)08609-6]

PACS number(s): 61.25.Em, 61.12.Ld

I. INTRODUCTION

The understanding of liquid state microscopic properties is one of the major tasks that are still open in the study of condensed matter. As the thermodynamic conditions are changed simple molecular liquids exhibit instabilities that lead to the well-known phase transitions. One is a second order transition to the vapor state, the other is a first order transition to the crystal phase. Of the two, the transition to the vapor state has been the object of an intense theoretical and experimental investigation, but the melting transition has received considerably less attention. The rapid variation of the one-particle density, which is uniform in the liquid and in the vapor phases, and becomes highly structured in the solid phase, causes formal difficulties in the application of the current theories to such a phase transition.

Among the various theoretical methods that can be applied to the study of the melting transition, the density-functional approach appears to be powerful enough to allow quantitative predictions and simple enough to maintain the qualitative picture. The input requested by this theory is a detailed knowledge of the microscopic structure and of the thermodynamic functions of the homogeneous (liquid) phase [1]. In this framework, model systems can play a very effective role. In fact, the freezing parameters of a classical hard-sphere fluid, obtained from density-functional theory, agree with the simulation results to within a few percent [2,3].

An interesting issue is the extension of the theoretical methods to quantum systems and the understanding of the physical nature of the freezing transition in quantum liquids. The reformulation by Haymet and Oxtoby [4] of the original Ramakrishnan and Yussouff approach [5], in terms of the density-functional theory, has been recently extended to quantum systems and applied to the freezing of a Lennard-Jones model of ^{4}He at finite temperature [6]. A different version of the method, namely, the modified weighted-density approximation [7–9] has also been extended to quantum systems and applied to the freezing of a Bose liquid of hard spheres at zero temperature [10]. Again, the necessary input of the theory is the structural and thermodynamic information on the corresponding quantum liquid.

There are, however, two fundamental issues to be dealt with before these theories can be fully accepted. One is related to the role of the attractive forces in the intermolecular interactions and the other is a detailed knowledge of the extent to which these methods can be extended to the domain of real quantum systems. Since the attractive part of the interatomic potential of helium is quite small, the hydrogen isotopes come immediately to mind as meaningful test cases. Another interesting feature of liquid hydrogens is their large compressibility. In fact, for these liquids, it is possible to span a density range of about a factor of 2 (e.g., on the 31-K isotherm of $^1H_2$) between the liquid-vapor coexistence line and the liquid-solid transition. However, not much has been learned about the microscopic structure of liquid hydrogen from either x-ray or neutron diffraction experiments [11], while only recently reliable measurements of $S(Q)$ have been obtained for gaseous [12] and liquid [13,14] deuterium.

One reason for the scarcity of neutron diffraction data of liquid hydrogen is the role played by the so-called inelasticity effects. Basically, these result from the recoil of the target nucleus in the scattering event. The inelasticity effects are larger for systems composed of light molecules and, therefore, the correction procedure first introduced by Placzek [15] cannot be applied to systems whose molecular mass is comparable with that of the neutron. The way the inelastic scattering affects the diffraction pattern, and how the experimental data can be corrected for it, has been the object of much work [16]. Such corrections are obviously more difficult in molecular systems than in monatomic.

Besides the inelastic correction problem, neutron diffraction experiments on liquid hydrogen remain extremely difficult, due to the unfavorable ratio of the coherent (internuclear) to the incoherent (self) neutron scattering cross sections. The situation is much better for deuterium, whose nuclear coherent cross section is larger than the incoherent one. Moreover, the effects of the inelasticity corrections are smaller due to the higher mass ratio of this nuclide with respect to the neutron. Therefore, deuterium becomes an ideal candidate for neutron diffraction studies of quantum liquids.

Recently, diffraction experiments in fluid deuterium have

been performed in the critical region [12] and in the vicinity of the triple point [13,14]. The experimental results in the gas phase have been compared with quantum path integral Monte Carlo (PIMC) simulations of a Lennard-Jones system [17]. Refined experimental data in the liquid phase have shown a remarkable agreement with PIMC simulations using a more accurate potential [18].

As we have already mentioned, the experimental determination of the microscopic structural information in the vicinity of the melting line is of great importance for establishing a theoretical framework for the freezing transition. Therefore, in order to extend the available structural data of liquid deuterium to higher pressures, we have performed a diffraction experiment in the compressed liquid phase. We decided to span the thermodynamic region of liquid deuterium in the vicinity of the liquid-solid coexistence line within a range of pressures between 50 and 500 bars, and in a temperature interval between 20.7 and 29.0 K. Due to the high compressibility of deuterium, a density variation of about 10% can be obtained in the liquid reaching, at the highest pressure, a density very close to that of the solid at the triple point. The corresponding molecular number density range is between 26.47 and 29.03 nm^{-3}. For the sake of comparison, at the triple point, the density of the liquid is 25.99 nm^{-3} and that of the solid is 29.39 nm^{-3}.

This paper reports on the precise experimental determination of the static structure factor of liquid deuterium in a large pressure range and in the region of the liquid phase close to the melting phase transition. In Sec. II we describe the experimental details, while in Sec. III we give a general description of the data analysis. The determination of the intermolecular structure factor and its variation with the thermodynamic conditions will be the subject of Sec. IV. Section V will be devoted to the discussion of the results.

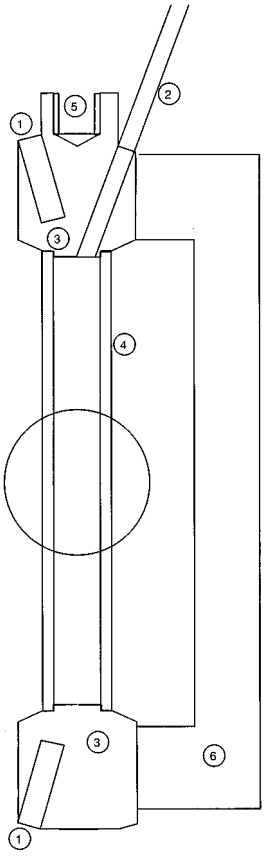

FIG. 1. Schematic drawing of the scattering cell. 1: temperature sensor holes; 2: 1/16 in. SS316 pipe for gas filling; 3: top and bottom copper caps; 4: vanadium tube (inside diameter 10 mm, wall thickness 2 mm); 5: threaded hole for holding the sample; 6: copper bypass. The circle in the middle of the figure represents the cross section of the neutron beam.

II. EXPERIMENTAL DETAILS

The experiment has been performed on the Small Angle Neutron Diffractometer for Amorphous and Liquid Samples (SANDALS) at the spallation neutron source ISIS of the Rutherford Appleton Laboratory (UK). The measurements were carried out along similar lines as in the previous (low pressure) experiment on liquid deuterium, which is described in Ref. [13]. However, some of the details are different and will be described more thoroughly.

Because of the larger pressure range involved in the present experiment, a stronger vanadium container was manufactured. This was obtained from a vanadium tube (10-mm internal diameter, 79-mm height, and 2-mm wall thickness) welded on either side of a copper cap. The container was mounted on the cold finger of a temperature-controlled helium closed-cycle refrigerator. Two calibrated Rh-Fe resistance thermometers were fitted in holes located in the top and bottom caps, and a welded 1/16 in. steel tube (SS316) connected the interior of the container with the external gas handling system. The overall design of the scattering cell is reported in Fig. 1. Due to the low thermal conductivity of vanadium, a copper bypass was inserted, out of the neutron path, between the two end flanges of the container. The pressure was measured by means of a calibrated gauge transducer and the density was derived by means of the equation of state given by Prydz [19]. This gives the density in the liquid phase with an overall accuracy of 0.3% below 100 atm. No estimation of accuracy is reported for higher pressures, but no other thermodynamic data are available. Therefore, we have used the Prydz equation of state in the whole range of pressures investigated. The thermodynamic coordinates of the five points where we have carried out the experiment are given in Table I. In the following, we will refer to the various thermodynamic states by means of the labels reported in the first column of Table I. Figure 2 shows the thermodynamic coordinates of the present and previous neutron diffraction experiments in deuterium.

For each thermodynamic point four independent subruns (equivalent to an integrated proton current of ISIS of 400 μA h each) were executed in order to check the stability of both the sample and the experimental setup. In addition, an empty-container run of similar total length was carried out at the beginning and at the end of the experiment, in order to check the long-term stability of the counting electronics and of the instrumental background. The instrumental and sample stabilities were found to be very good and compared well with the previous experiment on liquid deuterium (see Fig. 3 of Ref. [13]). The empty-container run (vanadium) was also used for calibration purposes and, to this aim, a background run was carried out with the vanadium container

TABLE I. The thermodynamic parameters of the experiment. The equation of state and the compressibilities are obtained from Ref. [19]. The thermodynamic conditions of the triple point (TP) are also reported for convenience.

Label	T/K[a]	p/bar[b]	n/nm^{-3}	$S(0)$
1	20.7	48.5	26.47±0.05	0.0606
2	22.0	136	27.67±0.05	0.0445
3	24.0	208	28.02±0.04	0.0374
4	26.0	330	28.67±0.04	0.0299
5	29.0	467	29.03±0.03	0.0269
TP	18.71	0.171	25.99[c]	
	18.71	0.171	29.39[d]	

[a]The estimated uncertainty in the temperature is $\Delta T = 0.5$ K.
[b]The average fluctuation of the measured pressure was below $\Delta P = 0.1$ bar, however we estimated an uncertainty $\Delta P = 1$ bar in the absolute reading.
[c]Density of the liquid phase.
[d]Density of the solid phase.

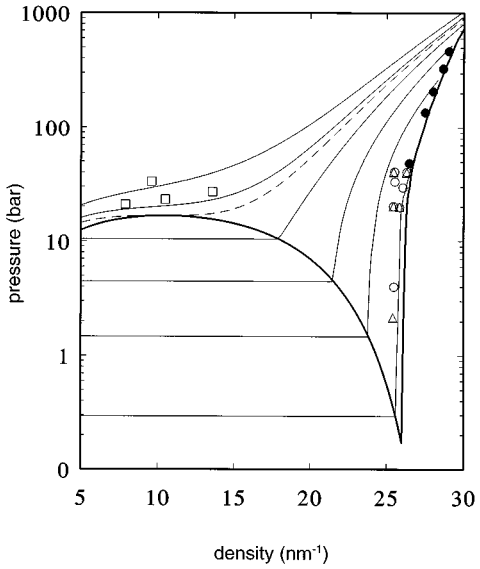

FIG. 2. A mapping of the thermodynamic coordinates where neutron scattering diffraction experiments have been performed on deuterium. The full lines are the isotherms at 20, 25, 30, 35, 40, and 45 K. The bold lines are the coexistence (liquid-vapor) and melting curves. The dashed line is the critical isotherm at $T = 38.34$ K. The black dots refer to the present experiment. The triangles and the circles are the results of Refs. [13] and [14]. The squares are relative to Ref. [12].

moved out of the neutron beam.

The time-of-flight (TOF) diffraction patterns were recorded by ten independent detector banks, placed at the scattering angles $\theta = 21.10°$, 18.09°, 16.23°, 14.61°, 13.08°, 11.79°, 9.23°, 6.75°, 5.02°, and 3.87°. The range of incident neutron energies used was between 0.5 and 4 eV.

III. DATA ANALYSIS

The usual corrections for background and container scattering, self-shielding, absorption, and multiple scattering were taken into account by means of the standard routine package ATLAS [20]. For each scattering angle, the final scattering cross section (per molecule) was normalized to absolute units by using the empty can, which is made of pure vanadium, as a reference system. In this way, any possible error in positioning the reference vanadium sample was avoided.

The problem of dealing with the inelasticity corrections has been already analyzed in Ref. [13], and the same conclusions apply to the present experiment. Simple calculations, based on a monatomic ideal gas model, can be carried out in order to evaluate the magnitude of the inelasticity corrections, which should be applied to the TOF spectra of deuterium. The results appear quite sensitive both to the mass of the monatomic model (either 2 or 4) and to the value of the scattering angle. If the scattering angles are kept below 20°, the effect of the corrections can be summarized as follows. In the Q region beyond 30–40 nm^{-1} the correction term is almost constant, while in the limit $Q \to 0$ it diverges. Correspondingly, in the low-Q limit of the experimental spectra, one observes a clear, unphysical, rise of the diffraction intensity. In the intermediate region, $Q = 10-30$ nm^{-1} some structure appears, which is induced by the energy spectrum of the incident neutrons, but in any case it remains below 1% with respect to the constant background correction (cf. Fig. 2 of Ref. [13]). Since the overall accuracy of our diffraction data was estimated to be of the order of 1%, we have decided to neglect the inelasticity corrections, at this stage, and combine them into the background subtraction that is described in the following paragraphs.

By assuming that the diatomic molecule of deuterium can be described by a rigid rotor model, the differential scattering cross section is [14,21]

$$d\sigma/d\Omega = u(Q)[S(Q)-1] + \nu(Q), \tag{1}$$

where Q is the momentum transfer and the functions $u(Q)$ and $\nu(Q)$ are the molecular form factors. $S(Q)$ is the static structure factor of the molecular centers of mass. The functions $u(Q)$ and $\nu(Q)$ are interpreted, respectively, as the *intermolecular* and *intramolecular* neutron cross sections. Equation (1) neglects orientational correlations, which is a reasonable assumption for D_2 in the present conditions [22]. Within the rigid rotor model, the expressions for the molecular form factors $u(Q)$ and $\nu(Q)$ have a very simple analytical form [21]:

$$u(Q) = 4a_{\mathrm{coh}}^2[\sin(\beta)/\beta]^2, \tag{2}$$

and

$$\nu(Q) = 2(a_{\mathrm{coh}}^2 + a_{\mathrm{inc}}^2) + 2a_{\mathrm{coh}}^2 \sin(2\beta)/(2\beta), \tag{3}$$

where $\beta = Qd/2$. Here d is the (fixed) distance between the two nuclei and a_{coh} and a_{inc} are the bound-atom scattering amplitudes for the deuterium nuclide.

As the neutron energy of a conventional thermal source is usually lower than the vibrational gap, the rigid rotor approximation would appear appropriate in this case. However, pulsed sources produce neutrons whose energy distribution easily exceeds many eV. As the energy of the vibrational

transition of the deuterium molecule is 0.386 eV, it appears that the rigid rotor model may become inadequate. Therefore, this simple model has been generalized in order to take into account the vibrational motion of the molecule. The new expressions for the intermolecular and intramolecular cross sections of deuterium, $u(Q)$ and $\nu(Q)$, have been obtained for a freely rotating harmonic oscillator model [23]. The result of the theoretical calculation is given as a sequence of functions that approximate the true behavior. To the lowest-order approximation the solutions are

$$u^{(0)}(Q)=4a_{\mathrm{coh}}^2[\exp(-\alpha^2/2)\sin(\beta)/\beta]^2 \tag{4}$$

and

$$\nu^{(0)}(Q)=2(a_{\mathrm{coh}}^2+a_{\mathrm{inc}}^2)+2a_{\mathrm{coh}}^2[\exp(-2\alpha^2)\sin(2\beta)/(2\beta)], \tag{5}$$

where now $\beta=Qd_e/2$ and $\alpha=Q(\hbar/2M\omega_v)^{1/2}$. Here M, ω_v, and d_e are the molecular mass, the angular frequency of the molecular vibrational transition, and the *equilibrium* distance of the two nuclei, respectively. In Eq. (5), the coefficient of the oscillating term holds for a normal ortho-para composition and its theoretical value is 0.891 barn. For pure ortho-deuterium this coefficient changes to 0.972. It is immediately recognized that Eqs. (4) and (5) represent the familiar rigid rotor solution modulated by a Debye-Waller factor. The sequence is shown to converge after a few iterations and it is found that the limit functions can be well approximated by Eqs. (4) and (5) provided that the molecular parameters are slightly changed with respect to their true values [23].

It could be discussed whether the simple harmonic oscillator model is sufficient, or a more sophisticated anharmonic model should be introduced, for describing the vibrational motion of the deuterium molecule. Of course, it is not easy to give an answer without carrying out the actual calculation. However, the fact that the exact solution of the harmonic model can be well represented by its zeroth order functional form by just changing very little the molecular parameters gives a positive indication on the subject. At any rate, we will assume that the present model holds until the precision of the experimental data provides evidence to the contrary. At present, as will be discussed in the following, no such evidence exists.

In order to derive the intermolecular structure factor, the intramolecular scattering has to be subtracted from the measured spectrum and a deconvolution from the molecular form factor must be carried out. However, as noted previously [13], this is a very delicate procedure, which implies the subtraction of some residual systematic error, including the inelasticity effects, possibly affecting the data after the standard correction procedure. Accordingly, for every scattering angle, and for each thermodynamic point, we have fitted the region $Q>80$ nm^{-1} (which is determined by the self-molecular term only), with a function

$$\nu^{(0)}(Q)=A+BQ+CQ^2 + D[\exp(-2\lambda_{\mathrm{DW}}^2Q^2)\sin(Qd_e)/(Qd_e)], \tag{6}$$

where the parameters A, B, C, and D were left free and the molecular parameters λ_{DW} and d_e were allowed to change in a limited interval (less than 1%) around their expected effective values $\lambda_{\mathrm{DW}}^2=1.3566\times10^{-5}$ nm^2 and $d_e=0.074104$ nm [23]. Therefore, the constant portion of the inelasticity corrections is included in the determination of the constant factor A. It turns out that the average value of A is 1.217 b sr^{-1} per molecule against a theoretical value of 1.214 for the incoherent scattering of the two deuterium nuclei. The parameters B and C, accounting for a possible curvature of the background level that is likely produced by a poor screening of the instrument for the fast neutrons, are 3 and 6 orders of magnitude smaller ($B\approx10^{-3}$ b sr^{-1} nm and $C\approx10^{-6}$ b sr^{-1} nm^2, per molecule, respectively). Thus, we find an almost insignificant deviation from a constant background level. This is mainly determined by the nuclear incoherent cross section and is only little affected by the inelasticity term (also constant).

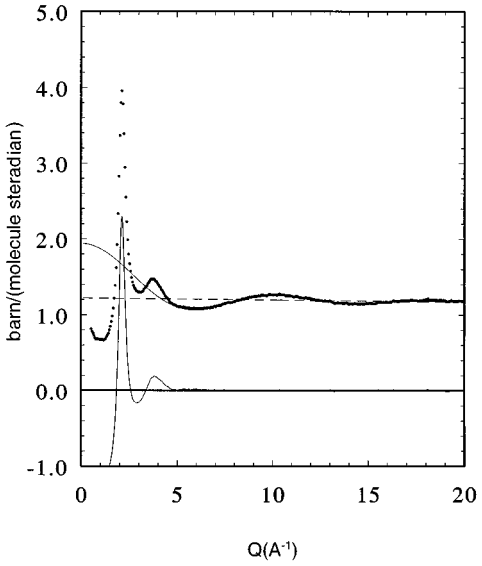

FIG. 3. Separation of the various contributions in the scattering cross section. The figure refers to the first spectrum (θ=21.10°) of the first run. The points are the experimental data, and the full line through the points is the fitted intramolecular contribution. The full line on the bottom of the figure is the intermolecular term (the product of the structure factor and of the molecular form factor).

IV. THE DERIVATION OF THE INTERMOLECULAR STRUCTURE FACTOR

For each thermodynamic point, we had ten different spectra, one for each detector bank. In turn, on every spectrum, the intramolecular contribution was determined by the fitting procedure outlined above. By subtracting this contribution from the measured cross section we obtained the intermolecular part, which corresponds to the first term of Eq. (1). Figure 3 shows, as an example, the separation of the various components relative to the first spectrum of the first run. Since no inelastic scattering correction was operated on the raw data (only the constant background contribution was included in the fitting procedure) we have analyzed the data for possible evidence of a trend in the parameter A [cf. Eq. (6)] as a function of the scattering angle. However, no such evidence was found.

By comparing the various intermolecular contributions a

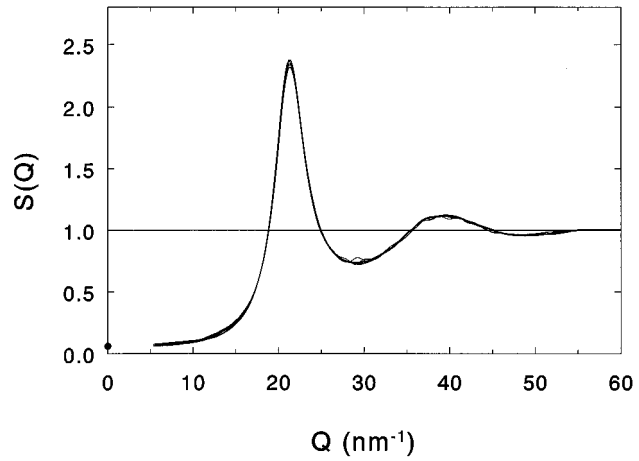

FIG. 4. The structure factor for the molecular center of mass of liquid deuterium. Spread of the results at different scattering angles after correcting the radial distribution function for systematic effects. The full dot represents the compressibility value. The data refer to state 1 of Table I.

general picture emerges. Spectra 1–7 (θ=21.10°, 18.09°, 16.23°, 14.61°, 13.08°, 11.79°, 9.23°) are in quite good agreement among themselves, and do not show any particular systematic trend. Conversely, the three lowest-angle spectra (θ=6.75°, 5.02°, and 3.87°) are not consistent with the

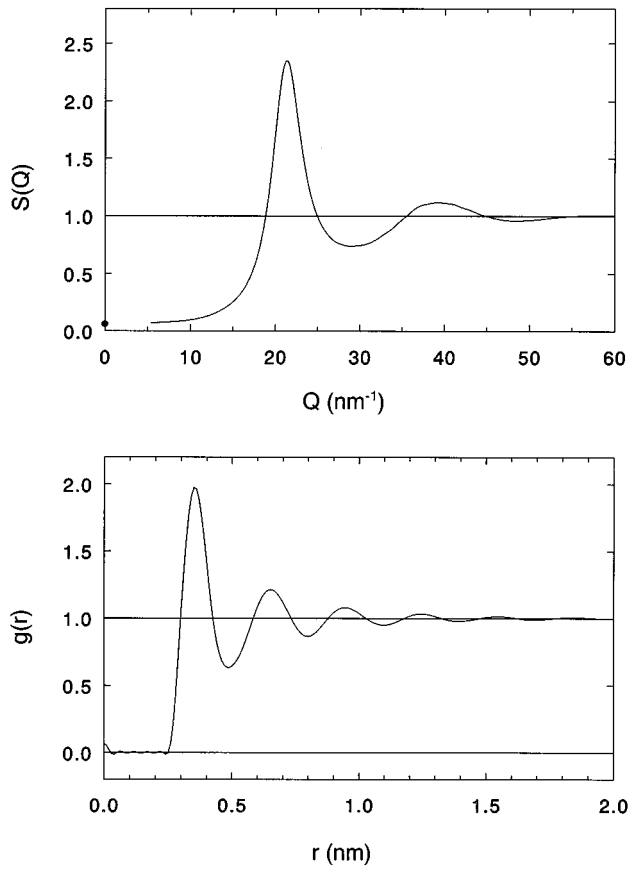

FIG. 5. Final determination of the structure factor (upper) and the radial distribution function (lower) for state 1 of Table I. The full dot in the upper graph represents the compressibility value.

others, nor among themselves. We attributed this behavior to the presence of a *sample dependent background*, which is more evident for the lower-angle banks, which happen to be closer to the neutron beam pipe [24]. In the following we will report only on the analysis of data carried out on the first seven spectra. Thus, as no evident trend was discovered as a function of the scattering angle, each spectrum was treated as an independent experimental determination of the intermolecular term. However, the differences found were greater than the combined statistical errors. In previous cases we found that by imposing strict physical constraints on the measured diffraction patterns, the various experimental determinations of the structure factor merged in a beautiful agreement, much better than the original data. The same procedure, described below, has been applied in this case.

For a fixed thermodynamic point, each measured diffraction pattern (corresponding to a different scattering angle) was first divided by the molecular term $u(Q)$. The resulting $S(Q)$ was then cut on either side in the noisy regions. On the low-Q side we have extrapolated the experimental function with a constant behavior starting from the minimum around $Q=10$ nm^{-1} (cf. Fig. 3). On the high-Q side, the function $S(Q)-1$ was set equal to 0 in the region beyond 60 nm^{-1}, where the divergence due to the zero of the molecular form factor made the experimental function extremely noisy. The function so obtained was then Fourier transformed to r space obtaining a trial radial distribution function $g(r)$. This shows unphysical oscillations at very low r. However, just cutting these oscillations does not help as this simple procedure influences the level and the amplitude of the back-transformed $S(Q)-1$. A much cleaner result is obtained if the resulting $g(r)-1$ is normalized in such a way to be consistent with the experimental isothermal compressibility. In this case (the normalization factor being 1.00 to within 2%), a much better agreement among the different spectra is recovered. As an example, Fig. 4 shows the spread of the seven independent determinations after the procedure for the first thermodynamic point. In Fig. 5 we report both the final determination of the intermolecular $S(Q)$ (averaged over the seven angles) and its Fourier transform $g(r)$. The data are still relative to the first thermodynamic point (cf. Table I). In Fig. 6 we report the final determinations of the intermolecular structure factor (center of mass) for the five measured points in the compressed liquid deuterium close to the melting line. The overall qualitative behavior appears quite similar. However, a shift of the principal peak toward higher Q is apparent as the density of the liquid increases.

The variation of $S(Q)$ with the thermodynamic state is more clearly appreciated in Fig. 7, where the differences between the center-of-mass structure factor at the higher densities and the one at the lowest density are plotted. These have the expected behavior based on the results of the previous experiment on low pressure liquid deuterium (cf. Fig. 6 of Ref. [13]). In fact, in the density and temperature range of that experiment, the variation of $S(Q)$ due to the density change at constant temperature is nearly an order of magnitude larger than that due to the temperature change at constant density. Therefore, also in the present experiment, we can expect the differences among the structure factor of the various states to be very similar in shape to the density derivative of $S(Q)$ at constant temperature.

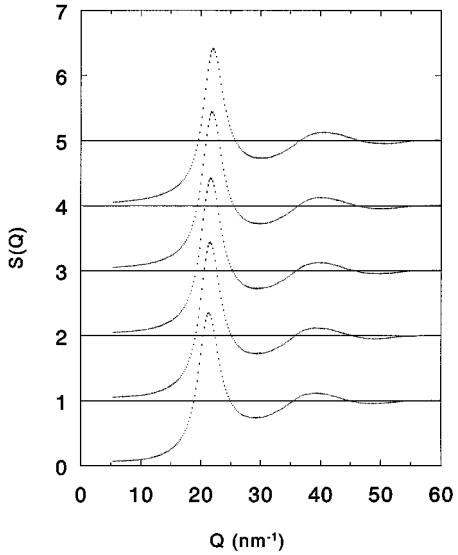

FIG. 6. Evolution of $S(Q)$ for deuterium as a function of the thermodynamic state. Only error bars are shown. Density increases from bottom to top (states 1 to 5 of Table I). The curves are shifted for clarity.

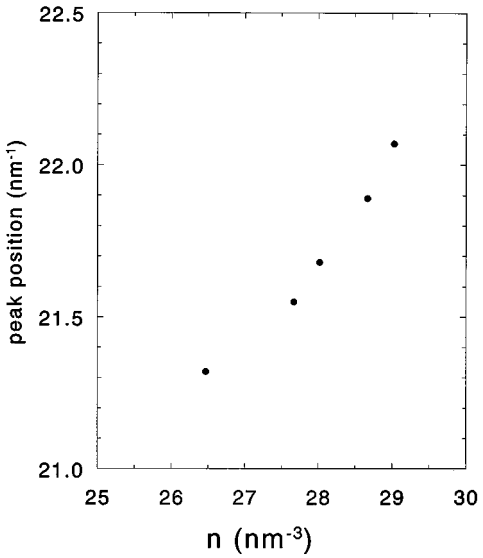

FIG. 8. Density evolution of the position of the main peak of $S(Q)$ for liquid deuterium. Even if the points are relative to different temperatures, the behavior is expected to be rather insensitive to temperature variations.

We repeat that the analysis of the data has been carried out by imposing physical constraints on the behavior of the center-of-mass radial distribution function. In particular, $g(r)$ vanishes identically at sufficiently short distances, and it reproduces the correct thermodynamic compressibility. We point out that no inelasticity correction was applied in the Q region considered here, apart from cutting the data below $Q=10$ nm^{-1} and subtracting a constant background. While this is rigorous for a monatomic ideal gas [13], the extension to a diatomic molecule cannot be considered more than a useful working hypothesis. However, the imposition of the physical constraints on the results should have reduced further the effects of this problem. As far as the change of $S(Q)$ with state point is concerned, the problem of the inelasticity corrections is easily circumvented. Both the intramolecular term of the cross section and the possible inelasticity correction should exhibit a weak dependence upon the thermodynamic state. Moreover, the density variation spanned by the present experiment is of the order of 10%. Therefore, we are confident that both factors effectively cancel in a differential analysis of the data.

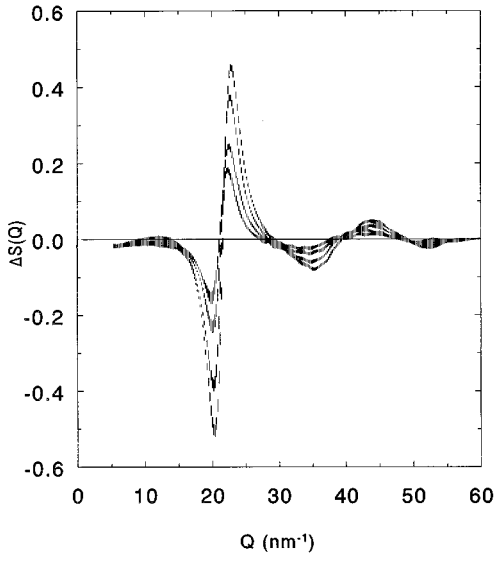

FIG. 7. Differences in the $S(Q)$ taking the lowest density point as a reference. Only error bars are shown. The differences increase with the density.

V. CONCLUSIONS

The intermolecular (center of mass) structure factor of liquid deuterium has been measured at five different thermodynamic points in the vicinity of the freezing transition. The points are within a pressure interval ranging from 48.5 to 467 bar, and a temperature interval between 20.7 and 29.0 K. The density variation is about 10%, ranging between 26.47 and 29.03 nm^{-3}. The density of the liquid, in the highest pressure conditions, is very close to the density of the solid phase at the triple point (cf. Table I). Therefore, a sensible variation of the structure factor was expected. This is actually observed in Fig. 6. In particular, the most striking effect that is apparent from the figure is the shift of the first peak of the $S(Q)$, toward higher Q, as density increases. This behavior is reported in Fig. 8.

The various experimental determinations have been obtained at different temperatures. However, it is expected that the peak position is rather insensitive to temperature variations. This is confirmed by the shape of the temperature derivative of $S(Q)$ [18]. Therefore, Fig. 8 gives an almost isothermal variation of the main peak position of the structure factor versus density.

The determination of the structure factor in an extended density range of the liquid phase is an important step in the development of the theory of freezing. For example, it will allow one to distinguish between a pure free-volume effect in

the isotropic phase and those produced by the long range correlations existing in the crystal phase. We expect that the present results will give new impulse to the theory of freezing in quantum liquids.

ACKNOWLEDGMENT

The technical assistance of the ISIS Instrumentation Division of RAL is gratefully acknowledged.

[1] For reviews of theoretical methods and applications see, for example, R. Evans, in *Liquids at Interfaces*, edited by J. Charbovin, J. F. Joanny, and J. Zinn-Justin (Elsevier, New York, 1989); D. W. Oxtoby, in *Liquids, Freezing and the Glass Transition*, edited by J. P. Hansen, D. Levesque, and J. Zinn-Justin (Elsevier, New York, 1991).
[2] A. D. J. Haymet, Prog. Solid State Chem. **17**, 1 (1986).
[3] M. Baus, J. Stat. Phys. **48**, 1129 (1987).
[4] A. D. J. Haymet and D. W. Oxtoby, J. Chem. Phys. **74**, 2559 (1981).
[5] T. V. Ramakrishnan and M. Yussouff, Phys. Rev. B **19**, 2775 (1979).
[6] J. D. McCoy, S. W. Rick, and A. D. J. Haymet, J. Chem. Phys. **90**, 4622 (1989).
[7] P. Tarazona, Mol. Phys. **52**, 81 (1984).
[8] W. A. Curtin and N. W. Ashcroft, Phys. Rev. A **32**, 2902 (1985).
[9] A. R. Denton and N. W. Ashcroft, Phys. Rev. A **39**, 4701 (1989).
[10] A. R. Denton, P. Nielaba, K. J. Runge, and N. W. Ashcroft, Phys. Rev. Lett. **64**, 1529 (1990).
[11] C. Andreani, J. C. Dore, and F. P. Ricci, Rep. Prog. Phys. **54**, 731 (1991).
[12] M. Zoppi, R. Magli, W. S. Howells, and A. K. Soper, Phys. Rev. A **39**, 4684 (1989).
[13] M. Zoppi, U. Bafile, R. Magli, and A. K. Soper, Phys. Rev. E **48**, 1000 (1993).
[14] E. Guarini, F. Barocchi, R. Magli, U. Bafile, M. C. Bellissent-Funel, J. Phys. Condens. Matter **7**, 5777 (1995).
[15] G. Placzek, Phys. Rev. **86**, 377 (1952).
[16] J. G. Powles, Mol. Phys. **36**, 1161 (1978); **36**, 1181 (1978).
[17] M. Neumann and M. Zoppi, Phys. Rev. A **44**, 2474 (1991).
[18] M. Zoppi, U. Bafile, E. Guarini, F. Barocchi, R. Magli, and M. Neumann, Phys. Rev. Lett. **75**, 1779 (1995).
[19] R. Prydz, NBS Report No. 9276, Boulder, CO, 1967 (unpublished).
[20] A. K. Soper, W. S. Howells, and A. C. Hannon, Rutherford Appleton Laboratory Report No. RAL-89-046, 1989 (unpublished).
[21] V. F. Sears, Can. J. Phys. **44**, 1279 (1966).
[22] J. Van Kranendonk, *Solid Hydrogen* (Plenum, New York, 1983).
[23] M. Zoppi, Physica B **183**, 235 (1993).
[24] Since the times of the experiment the problem has been thoroughly analyzed and a careful screening of the neutron beam pipe has been carried out, ending with an increase of the performance of the SANDALS diffractometer.